VERSITA

Cent. Eur. J. Chem. • 11(1) • 2013 • 116-122
DOI: 10.2478/s11532-012-0141-z

Central European Journal of **Chemistry**

Octahedral Cu^{II} and Ni^{II} complexes manifesting with *N*'-[1-(pyridin-2-yl)ethylidene] acetohydrazide: Structural outlooks and spectral characteristics

Research Article

Amitabha Datta[1*], Jui-Hsien Huang[1#], Jack K. Clegg[2],
Pei-Hsin Liu[1], Sheng-Jie Chuang[1]

[1]*Department of Chemistry, National Changhua University of Education,*
Changhua 50058, Taiwan

[2]*School of Chemistry and Molecular Biosciences,*
The University of Queensland, St. Lucia, QLD 4072, Australia

Received 23 August 2012; Accepted 6 September 2012

Abstract: A tridentate hydrazone precursor, *N*'-[1-(pyridin-2-yl)ethylidene]acetohydrazide (**L**) (1:1 refluxed product of acetichydrazide and 2-acetylpyridine), produced two octahedral Cu^{II} and Ni^{II} derivatives, $[CuL_2]\bullet NO_3$ (**1**) and $[NiL_2]\bullet ClO_4\bullet H_2O$ (**2**). Both are subjected to X-ray diffraction system, and structural investigation shows that the central metal atom (Cu^{II} or Ni^{II}) adopts a distorted octahedral geometry with N_4O_2 donor sets by coordination of a pair of independent hydrazone precursors. Besides X-ray study, IR and UV-vis spectra, thermal analysis and room temperature magnetic moments are utilized for establishing significant characteristics of both complexes. It is apparent that the M-N$_{pyridine}$ bonds are slightly longer than the M-N$_{imino}$ bonds, Cu1−N1 and Cu1−N4 [2.300(2) and 2.038(2) Å] for **1** and Ni1−N1 and Ni1−N4 [2.075(2) and 2.084(1) Å] for **2**, Cu1−N2 and Cu1−N5 [2.062(1) and 1.932(1) Å] for **1** and Ni1−N2 and Ni1−N5 [2.008(2) and 1.975(2) Å] for **2**, respectively. As per our observation, the effective magnetic moment value (μ_{eff}) is found to be 1.77 B.M. for **1** and 3.06 BM for **2**, respectively.

Keywords: *Copper(II) • Nickel(II) • Hydrazone • Spectral properties • Crystal structure*

1. Introduction

To get versatile coordination ability for a wide range of applications, like tridentate Schiff base precursors, hydrazone derivatives have been of substantial interest to inorganic chemists. Several transition metal complexes incorporating arylhydrazone precursors are used to produce effective models for clarification of mechanistic pathways of enzyme inhibited hydrazines [1] and a wide range of pharmacology and biochemistry applications [2]. Hydrazones consist of tri-atomic azomethines groups, C=N−N, and some of them show attractive features in the treatment of severe diseases, like tuberculosis [3]. This ongoing activity is very evident to form stable chelates containing transition metals that initiates different biological activities [4]. The potential of these hydrazone derivatives to reveal some characteristics, such as the ability to form metal-compounds possessing tridentate chelates [5-7]. Furthermore, these hydrazone derivatives exhibit keto-enol tautomerism and generate metal-complexes while behaving as a mono- or dianionic nucleating agent [8,9].

Aromatic hydrazide- and aroylhydrazone-containing transition metal complexes were explored earlier, [10-12] and we have noticed the participation of pyridine-2-carboxaldehyde during formation of tridentate blocking precursor [13]. The activity of these hydrazone containing metal-derivatives are very pronounced against gram-positive bacteria *in vitro*. This is very effective for the production of oral drugs among some genetic diseases,

---

* *E-mail: amitd_ju@yahoo.co.in*
# *E-mail: juihuang@cc.ncue.edu.tw*

like thalassemia [14]. The tridentate coordination potentiality of hydrazones facilitate bischelation with mono-nucleating substances consisting of an octahedral geometry of corresponding metal atoms [15].

As per our survey, aliphatic hydrazones are investigated less. We have reported earlier some aliphatic hydrazone derivatives of copper(II) [16-18]. In continuation of our research of tridentate hydrazone precursor mediated transition metal complexes, on our current contribution, two new octahedral complexes of Cu^{II} and Ni^{II}, $Cu[C_5H_4N\text{-}C(CH_3)\text{=}N\text{-}N\text{=}C(O)CH_3]_2•NO_3$ (**1**) and $Ni\{[C_5H_4N\text{-}C(CH_3)\text{=}N\text{-}N\text{=}C(O)CH_3][C_5H_4N\text{-}C(CH_3)\text{=}N\text{-}NH\text{-}C(O)CH_3]\}•ClO_4•H_2O$ (**2**) are explored and demonstrated systematically considering spectral and thermal features alongwith single crystal X-ray diffraction evaluation.

2. Experimental procedure

2.1. Materials

All chemicals handled during synthesis were of reagent grade. Acetichydrazide and 2-acetylpyridine (Aldrich), copper nitrate trihydrate and nickel perchlorate hexahydrate (Fluka) were purchased and subjected as commercially obtained.

2.2. Physical techniques

Elemental analyses were performed on a Heraeus CHN-OS Rapid Elemental Analyzer at the Instrument Center of the NCHU. Infrared spectra were recorded on a Perkin-Elmer 883-Infrared spectrophotometer in the range 4000–200 cm^{-1} as KBr pellets. Electronic spectra were measured on a Hitachi U 3400 (UV–Vis.–N.I.R.) spectrophotometer in methanol. Thermal analysis was carried out at a heating rate of 10ºC min^{-1} with a Mettler-Toledo Star TGA/SDTA-851e thermal analyzer system in a dynamic atmosphere of N_2 (flow rate 30 mL min^{-1}) in an alumina crucible for the range 25–350ºC. Magnetic susceptibility was measured on a powder sample in a vibrating sample magnetometer using mercury(tetrathiocyanato)cobaltate as the standard.

2.3. Preparation of the ligand

The ligand was synthesized by refluxing acetic hydrazide (0.740 g, 10 mmol) and 2-acetylpyridine (1.12 mL, 10 mmol) in 50 mL of methanol accordingly *via* previous literature [16]. The resultant yellow solution containing the tridentate precursor was used without additional purification. The proposed ligand displays keto-enol tautomerism, shown in Scheme 1.

2.4. Preparation of the complex $[CuL_2]•NO_3$ (1)

To a 20 mL methanol solution of copper nitrate trihydrate (0.241 g, 1 mmol), the hydrazone precursor (2 mmol) was added, stirred for sometime and allowed to sit untouched at room temperature. After a few days, dark brown colored and rectangular shaped crystals of **1** were produced. The shiny crystals were filtered off, washed with distilled water and air-dried. Yield: 79%. Anal. Calc. for $C_{18}H_{21}CuN_7O_5$: C, 45.14; H, 4.42; N, 20.47. Found: C, 45.38; H, 4.11; N, 20.58%.

2.5. Preparation of the complex $[NiL_2]•ClO_4•H_2O$ (2)

Complex **2** was generated ensuing the same procedure for **1**, only using nickel perchlorate hexahydrate (0.365 g, 1 mmol) as the metal salt. Yield: 79%. Anal. Calc. for $C_{18}H_{23}NiClN_6O_7$: C, 40.83; H, 4.38; N, 15.87. Found: C, 40.62; H, 4.23; N, 16.04%.

2.6. X-ray crystallography

Data were collected with an Oxford Gemini Ultra employing either confocal mirror monochromated Cu-K_{α} radiation generated from a sealed tube (1.5418 Å) or graphite monochromated Mo-K_{α} radiation generated from a sealed tube (0.71073 Å) with ω and ψ scans at 120(2) K. Data integration and reduction were undertaken with CrysAlisPro [19] and subsequent computations were carried out using the WinGX-32 graphical user interface [20]. Gaussian and empirical absorption corrections were applied using CryAlisPro [19]. Structures were solved by direct methods using SHELXS-97 [21], then refined and extended with SHELXL-97 [22]. A total of 6483 for **1** and 12697 for **2**, reflections were collected, from which 3690 (**1**) and 4820 (**2**) independent [R(int) = 0.0193 and 0.0327, respectively] reflections were measured. $R1 = \Sigma||F_o| - |F_c||/\Sigma|F_o|$ for $F_o > 2\sigma(F_o)$; $wR2 = (\Sigma w(F_o^2 - F_c^2)^2/\Sigma(wF_c^2)^2)^{1/2}$ all reflections $w = 1/[\sigma^2(F_o^2) + (0.0438P)^2 + 0.9753P]$ for **1** and $w = 1/[\sigma^2(F_o^2) + ((0.0341P)^2 + 1.2813P]$ for **2**, respectively, where $P = (F_o^2+2F_c^2)/3$. In general, non-hydrogen atoms with occupancies greater than 0.5 were refined anisotropically. Carbon-bound hydrogen atoms were included in idealized positions and refined using a riding model. Oxygen-bound hydrogen atoms were first located in the difference Fourier map before refinement with bond length and angle restraints. Details concerning crystal data, data collection characteristics and structure refinement are summarized in Table 1.

Table 1. Crystallographic data of **1** and **2**.

	1	**2**
Empirical formula	$C_{18}H_{21}CuN_7O_5$	$C_{18}H_{23}NiClN_6O_7$
Formula weight	478.96	529.58
Temperature (K)	120(2)	120(2)
Wavelength (Å)	0.71073	0.71073
Crystal system	Triclinic	Monoclinic
Space group	P-1	P2(1)/c
a, Å	7.9195(5)	8.0693(3)
b, Å	10.5897(7)	19.1709(7)
c, Å	13.5736(9)	14.9031(6)
α, deg	110.489(6)	90
β, deg	96.451(5)	104.613(4)
γ, deg	105.579(6)	90
Volume, Å^3	999.94(13)	2230.87(15)
Z	2	4
Density, mg m^{-3}	1.591	1.577
Absorption Coefficient, mm^{-1}	1.967	1.043
F(000)	494	1096
Crystal size, mm^{-3}	0.22×0.14×0.13	0.24×0.18×0.17
θ range for data collection	3.38−25.05	3.33−30.75
Reflections collected	6483	12697
Independent reflections	3690 [*R(int)* = 0.0193]	4820 [*R(int)* = 0.0327]
Data / restraints / parameters	6483 / 0 / 284	12697 / 0 / 306
Final R indices [I>2σ(I)]	*R1* = 0.0335, *wR2* = 0.0877	*R1* = 0.0405, *wR2* = 0.0900
R indices (all data)	*R1* = 0.0346, *wR2* = 0.0884	*R1* = 0.0567, *wR2* = 0.0995
Largest diff. Peak and hole, e Å^{-3}	0.490 and -0.688	0.602 and -0.742

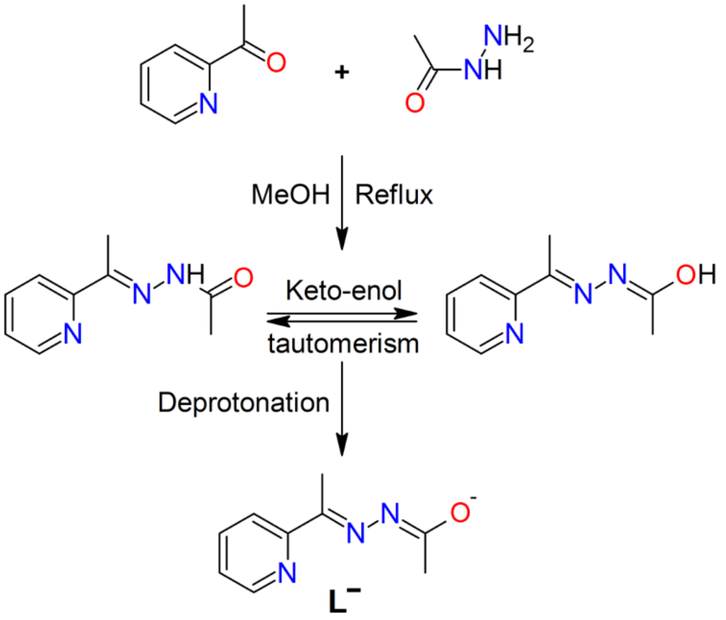

Scheme 1. Keto-enol tautomerism of the proposed ligand.

3. Results and discussion

3.1. Infrared spectra

The IR spectrum of **1** shows a C–O absorption band at 1093 cm^{-1} for **1** and 1087 cm^{-1} for **2**, respectively due to deprotonation of the hydrazone precursor whereas it emerges at 1654 cm^{-1} as free substrate. IR absorption bands at 1576 and 1562 cm^{-1} for **1** and **2**, respectively can be designated as C=N stretching frequency of metal-bound precursor [23], while subjecting before complexation, the band is ascertained at 1681 cm^{-1}. The different coordination modes in metal complexes show stretching frequencies 426 and 317 cm^{-1} for **1**, 467 and 348 cm^{-1} for **2**, respectively which is allocated to $\nu_{(M–N)}$ and $\nu_{(M–O)}$ in concern. Furthermore, intense bands at 647 and 419 cm^{-1} for **1** and 635 and 409 cm^{-1} for **2**, respectively are observed due to in plane and out of plane oscillations of low energy pyridine ring while remains as free, but drifted to higher regions, at 680–715 for **1** and 421-426 cm^{-1} for **2**, during complex formation.

3.2. Electronic spectra

We have measured electronic spectra by using HPLC grade acetonitrile. Distinguishable absorption bands at 219 and 278 nm are observed that correspond $\pi\rightarrow\pi^*$ transition within the hydrazone precursor [24]. It is noticeable that shifting of $n\rightarrow\pi^*$ transition of azomethine part to lower frequencies on metal coordination, whereas, as free precursor it appears at 465–325 nm [24]. The corresponding LMCT band for **1** is identified at 385 nm. While illustrating three spin-allowed d–d transitions in **2**, appeared at 244, 381, and 637 nm, it could be referred as $3T_{2g}(F) \leftarrow 3A_{2g}(F)$, $3T_{1g}(F) \leftarrow 3A_{2g}(F)$, and $3T_{1g}(P) \leftarrow 3A_{2g}(F)$, a recognition in increased energy level. As per previous references [25,26], bands cited within a region of 300–450 nm, could be allocated as $\pi\rightarrow\pi^*$ transition of azomethine chromophore whereas the corresponding bands at 200–300 nm, preferably indicates $\pi\rightarrow\pi^*$ transition of pyridine ring.

3.3. Thermal analysis

The thermal decomposition for compounds **1** and **2** were carried out and analyzed. The thermo gravimetric investigation shows that complex **1** is stable up to ~230ºC and then proceeds to decompose in two temperature ranges, 235-255ºC that is consistent with the loss of nitrate anion present in the lattice; and 260-310ºC that conforms the loss of hydrazone precursor. Similarly, the complex **2** is stable up to 245ºC, soon after achieving the temperature range, 250-265ºC, it decomposes due to the loss of lattice water molecule; followed by subsequent mass loss on 270-295ºC for perchlorate anion. Finally the mass loss between the temperature range of 300-345ºC, is consistent with the dissociated hydrazone.

Table 2. Selected bond lengths [Å] and angles [°] for **1**.

Cu1-N1	2.300(2)	Cu1-N2	2.062(1)
Cu1-N4	2.038(2)	Cu1-N5	1.932(1)
Cu1-O1	2.388(14)	Cu1-O2	1.989(13)
N2-N3	1.375(2)	N5-N6	1.384(3)
N3-C8	1.362(3)	N6-C17	1.332(2)
N2-C6	1.291(3)	N5-C5	1.290(3)
C8-O1	1.227(2)	C17-O2	1.279(2)
N1-Cu1-O1	146.26(6)	N2-Cu1-N5	177.63(7)
N4-Cu1-O2	159.07(7)	O2-Cu1-N5	79.28(7)
N1-Cu1-N2	73.98(6)	O1-Cu1-N2	72.32(6)
N4-Cu1-N5	79.83(7)	O1-Cu1-N4	89.64(6)
N1-Cu1-O2	93.41(6)		

3.4. Magnetic moment

The effective magnetic moments (μ_{eff}) of complexes, **1** and **2** at room temperature were monitored subjecting polycrystalline samples after modified diamagnetic corrections on Pascal's table. The effective magnetic moment value (μ_{eff}) is found as 1.77 B.M. for **1** and 3.06 BM for **2**, respectively, which is entirely compatible with anticipated spin only value of a $S = {}^1/_2$, d^9 copper(II) system for **1** and similarly for **2**, it resolves an evidence of Ni(II) (d^8) configuration possessing two unpaired electrons (S = 1).

3.5. Crystal structure

Fig. 1 represents the ORTEP of molecular geometry of **1** and corresponding bond lengths and angles are listed in Table 2. The copper atom belongs to N_4O_2 coordinated environment which has distorted octahedral geometry. Two units of hydrazone precursors belong to meridional orientation *via* NNO ($N_{pyridine}$, N_{imine} and $O_{acetoyl}$) donor sets and assembled two five-membered chelate rings. The Cu−$N_{pyridine}$ bond lengths [Cu1−N1 and Cu1−N4, 2.300(2) and 2.038(2) Å] are quite large than Cu−N_{imine} counterparts, [Cu1-N2 and Cu1-N5, 2.062(1) and 1.932(1) Å]. The N2−C6 and N5−C15 bond lengths [1.291(3) and 1.290(3) Å] are symptomatic of (C=N) double bonds. Considering the {= N–N=C(O^-)–} moiety, the corresponding two sets of bond lengths are [N−N (1.384(3), N–C (1.332(2) and C–O (1.279(2) Å] and [N−N (1.375(2), N–C (1.362(3) and C–O (1.227(2) Å] which conforms the involvement of both 'enolate' and

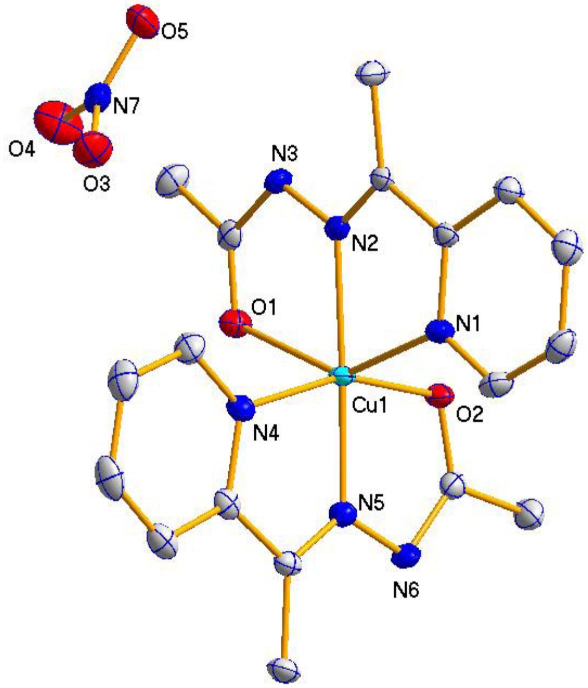

Figure 1. An ORTEP plot of complex **1**. Ellipsoids are drawn from 30% probability label. Hydrogen atoms are omitted for clarity.

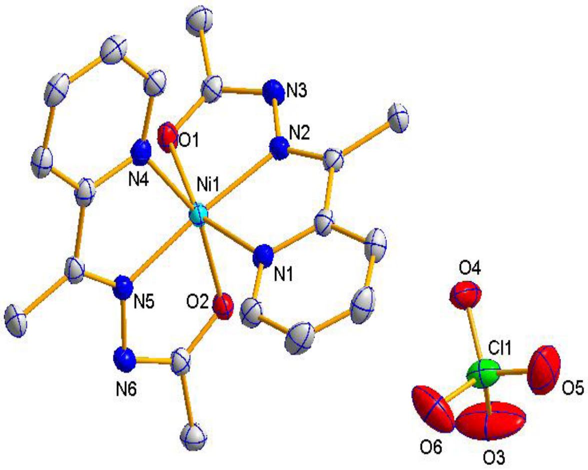

Figure 2. An ORTEP plot of complex **2**. Ellipsoids are drawn from 30% probability label. Hydrogen atoms are omitted for clarity.

‘keto’ form of pair of hydrazone units. A conventional Jahn-Teller distortion of CuN_4O_2 pseudo octahedron is revealed while countering the bond lengths and angles, shown in Table 2. The angles functioning the atoms at *trans* are 146.26(6)–177.63(7)° but those corresponding at *cis* alter from 72.32(6)–79.83(7)°. The most acute angles involve the pair of nitrogen atoms in each precursor and the most obtuse angles imply the imine nitrogen of one precursor and the tertiary nitrogen of the rest. The *cis* angles involving the oxygen atoms [93.41(6) and 89.64(6)°] are close to 90.0°. The Cu–N$_{Pyridine}$ and Cu–N$_{imine}$ bond lengths are analogous to previously reported hydrazone mediated Cu(II) derivatives [2.020(5) and 1.924(4) Å] [27], [2.042(19) and 1.927(16) Å] [28], [2.028(2) and 1.929(19) Å] [29] and [2.023(16) and 1.932(16) Å] [30]. The nitrogen bound hydrogen atom behaves as hydrogen bond donor, interacting with nitrate anion in the lattice (N(3)H ··· O(5) 2.15 Å, 153.8°).

Table 3. Selected bond lengths [Å] and angles [°] for **2**.

Ni(1)-N(1)	**2.075(2)**	**Ni(1)-N(5)**	**1.975(2)**
Ni(1)-N(2)	2.008(2)	Ni(1)-O(1)	2.140(2)
Ni(1)-N(4)	2.084(1)	Ni(1)-O(2)	2.054(2)
N(2)-Ni(1)-N(1)	78.16(7)	N(5)-Ni(1)-O(1)	104.73(6)
N(1)-Ni(1)-N(4)	93.19(7)	N(4)-Ni(1)-O(1)	91.16(6)
N(5)-Ni(1)-N(1)	100.35(7)	O(2)-Ni(1)-N(4)	156.79(6)
N(1)-Ni(1)-O(1)	154.91(6)	N(5)-Ni(1)-N(4)	78.74(7)
O(2)-Ni(1)-N(1)	91.30(6)	N(2)-Ni(1)-O(2)	97.36(6)
N(2)-Ni(1)-N(4)	105.85(7)	N(5)-Ni(1)-O(2)	78.06(6)
N(5)-Ni(1)-N(2)	175.19(7)	O(2)-Ni(1)-O(1)	94.36(6)
N(2)-Ni(1)-O(1)	76.89(6)		

Fig. 2 displays the ORTEP of complex **2**. Ellipsoids are drawn from 30% probability level. Selected bond lengths and angles are projected in Table 3. Similar to **1**, the central Ni^{II} atom of complex **2** exhibits as a distorted octahedron that constructed by meridionally comprised two hydrazone precursors leaving an ‘interligand angle’ of 78.52(3)º. While the generation of six-coordinated sphere, two five membered chelate rings subsequently participate in the formation of the NiN_4O_2 pseudo octahedron. The Ni−N$_{pyridine}$ bond lengths [Ni1−N1 and Ni1−N4, 2.075(2) and 2.084(1) Å] are considerably longer than Ni−N$_{imine}$ bond lengths [Ni1-N2 and Ni1-N5, 2.008(2) and 1.975(2) Å] and well comparable with Cu−N$_{pyridine}$ and Cu−N$_{imine}$ bond lengths in **1**. The corresponding N2−C6 and N5−C15 bond lengths [1.293(3) and 1.291(2) Å] are declarative of the formation of C=N double bonds. The angles implying *trans* atoms belong in the range of 175.19(7)–154.91(6)º where as those resulting *cis* positions diverge from 105.85(7)–76.89(6)º. The interrelated Ni−N distances in **2** are well comparable with previous literatures, 2.101(2)–2.119(9) Å in $[Ni\{NH_2CH_2C(Me)NH\}(py)_2(NCS)_2]$, [31] 2.094(4)–2.146(4) Å in $Ni\{NH_2C(Me)_2CH_2NH\ (CHMe_2)\}_2(NCS)_2]$ [32] and 2.055(2)–2.191(2) Å in $[Ni\{EtNHCH_2CH_2NHEt\}_2(NCS)_2]$ [33].

4. Conclusion

In this article, we have demonstrated two new octahedral Cu^{II} and Ni^{II} derivatives by integration of a hydrazone precursor and X-ray diffraction analysis as well as different spectral, thermal and magnetic measurements. Single crystal structural observation reveals that the metal possesses a distorted octahedral geometry. Further studies will elucidate the mechanistic pathway and modification that corresponds to several applications among metal complexes of newly designed organic precursors.

Acknowledgements

The authors would like to acknowledge the National Science Council of Taiwan for financial assistance.

Supplementary material

Crystallographic data for structural analysis has been deposited to the Cambridge Crystallographic Data Center, bearing CCDC 862123 and 870540. Copies of this information may be obtained free of charge from the Director, CCDC, 12 Union Road, Cambridge, CB2 IEZ, UK (fax: +44-1223-336-033; e-mail deposit@ccdc.cam.ac.uk or http://www.ccdc.cam.ac.uk).

References

[1] M.F. Iskander, S.E. Zayan, M.A. Khalifa, L. El-Sayed, J. Inorg. Nucl. Chem. 36, 556 (1974)

[2] J.R. Merchant, D.S. Clothia, J. Med. Chem. 13, 335 (1970)

[3] I. Geubeur, M. Guekezian, L.H.S.A. Terra, M.C.B. Moraes, C.L. Lago, J.R. Matos, M.E.V. Suarez-Iha, Polyhedron 23, 2095 (2004)

[4] M.E. Hossain, M.N. Alam, M.A. Ali, M. Nazimuddin, F.E. Smith, R.C. Hynes, Polyhedron 15, 973 (1996)

[5] M. Carcelli, S. Ianelli, P. Pelagatti, G. Pelizzi, Inorg. Chim. Acta 292, 121 (1999)

[6] G.G. Mohamed, Z.H.A. El-Wahab, J. Thermal Anal. Calorimetry 73, 347 (2003)

[7] Y. Song, Y. Xu, D.-R. Zhu, X.-Z. You, Acta Crystallogr. C56, 430 (2000)

[8] G.F. de Sousa, C.A.L. Filgueiras, A. Abras, S.S. Al-Juaid, P.B. Hitchcock, J.F. Nixon, Inorg. Chim. Acta 218, 139 (1994)

[9] D. Wester, G.J. Palenik, Inorg. Chem. 15, 755 (1976)

[10] B. Samanta, J. Chakraborty, D.K. Dey, V. Gramlich, S. Mitra, Struct. Chem. 18, 287 (2007)

[11] S. Sen, S. Mitra, D.L. Hughes, G. Rosair, C. Desplanches, Polyhedron 26, 1740 (2007)

[12] X.-S. Tai, F.-Y. Kong, Z. Kristallogr. 221, 341 (2006)

[13] N. Galic, B. Peric, B. Kojic-Prodic, Z, Cimerman, J. Mol. Struct. 559, 187 (2001)

[14] J.D. Ranford, J.J. Vittal, Y. Wang, Inorg. Chem. 37, 1226 (1998)

[15] S. Sen, P. Talukder, G. Rosair, S. Mitra, Struct. Chem. 16, 605 (2005)

[16] A. Datta, K. Das, Y.-M. Jhou, J.-H. Huang, H.M. Lee, Acta Crystallogr. E66, m1271 (2010)

[17] A. Datta, K. Das, Y.-M. Jhou, J.-H. Huang, H.M. Lee, Acta Crystallogr. E67, m123 (2011)

[18] K. Das, A. Datta, C. Sinha, J.-H. Huang, E. Garribba, C.-S. Hsiao, C.-L. Hsu, ChemistryOpen 1, 80 (2012)

[19] CrysAlisPro, Agilent Technologies Ltd, 1.171.35.11 2009

[20] L.J. Farrugia, J. Appl. Cryst. 32, 837 (1999)

[21] G.M. Sheldrick (1997), SHELXS-97. Program for Crystal Structure Resolution (Univ. of Göttingen, Göttingen, 1997)

[22] G.M. Sheldrick (1997), SHELXL-97. Program for Crystal Structures Analysis (Univ. of Göttingen: Göttingen, 1997)

[23] K. Nakamoto, Infrared and Raman Spectra of Inorganic and Coordination Compounds, Parts A and B, 5th edition (John Wiley, New York, 1997)

[24] A.B.P. Lever, Inorganic Electronic Spectroscopy, 2nd edition (Elsevier, New York, 1984)

[25] R.C. Felicio, E.T.G. Canalheiro, E.R. Dockal, Polyhedron 20, 261 (2001)

[26] S. Zolezzi, A. Decinti, E. Spodine, Polyhedron 18, 897 (1999)

[27] S. Sen, S. Mitra, D.L. Hughes, G. Rosair, C. Desplanches, Inorg. Chim. Acta 360, 4085 (2007)

[28] A. Ray, S. Banerjee, R.J. Butcher, C. Desplanches,

S. Mitra, Polyhedron 27, 1409 (2008)

[29] N.R. Sangeetha, S. Pal, Polyhedron 19, 1593 (2000)

[30] S. Banerjee, S. Sen, S. Basak, S. Mitra, D.L. Hughes, C. Desplanches, Inorg. Chim. Acta 361, 2707 (2008)

[31] K.M.A. Malik, S. Mitra, R.K.B. Singh, J. Chem. Crystallogr. 29, 877 (1999)

[32] C. Pariya, S. Ghosh, A. Ghosh, M. Mukherjee, A.K. Mukherjee, N.R. Chaudhuri, J. Chem. Soc. Dalton Trans. 337 (1995)

[33] C. Pariya, A. Ghosh, N.R. Chaudhuri, S. Ghosh, M. Mukherjee, A.K. Mukherjee, Polyhedron 15, 1643 (1996)